Computer models of a new deoxy-sickle cell hemoglobin fiber based on x-ray diffraction data

Xiang-Qi Mu and Beatrice Magdoff Fairchild
College of Physicians & Surgeons, Columbia University, and St. Luke's/Roosevelt Hospital Center, New York, New York 10025 USA

ABSTRACT A new x-ray fiber diffraction pattern from deoxygenated sickle cell erythrocytes has been observed. It displays 14 layer lines with a 109 Å periodicity compared with the 64 Å periodicity of the "classic" sickle cell hemoglobin (HbS) fiber. These data and association energy calculations serve as a basis for computer model building. Systematic searches over four-dimensional parameter space yielded twelve protofilament models that satisfy the following constraints: (*a*) two HbS molecules be related by twofold screw symmetry with a translational repeat of 109 Å; (*b*) at least one of the substituted residues in HbS, val β6, should participate in intermolecular contacts; and (*c*) the energy of intermolecular interaction be < -24 kcal/mol. Each of the protofilament models is a zigzag mono-strand that stands in contrast to the double-stranded protofilament of the "classic" fiber.

Fiber models were constructed with each of the 12 protofilament models, pseudo-hexagonally packed. Searches of variable packing parameters showed four fiber models with minimal protofilament association energies and minimal differences between calculated transforms and observed data. The *R*-factor was < 0.24 for each of these four models. In three of the fiber models the protofilament association energy is between $-$(93 and 130) kcal, and in a fourth, the energy is -64 kcal. One protofilament model constituted three distinct fiber models of the lower energy class, and a second protofilament model packed with a higher association energy into a fourth fiber model. The selection of a unique fiber model from among these four cannot be made because of the limited available data. Fibers models constructed with any of the ten other protofilament models do not satisfy the conditions of minimal association energy and *R*-factor.

INTRODUCTION

Sickle cell hemoglobin (HbS) differs from normal human hemoglobin in a substitution of val for glu at the two β6 positions of the molecule. This leads to a markedly diminished solubility of the unliganded molecule (1–3) that under appropriate conditions of temperature, pH, and concentration results in a molecular assembly into regular fibers.

The structure of the fibers has been studied extensively by image reconstruction of electron micrographs and by x-ray diffraction techniques. Through image reconstruction (4–6), the architectural characteristics, the approximate number of molecules in the helical repeat, and the number of strands in the fiber were determined. Compelling evidence derived from comparisons of x-ray diffraction patterns of fibers (7, 8) to crystalline deoxy-HbS, whose structure is known to 2.8 Å resolution (9–11), led to an identification of the fiber's basic structural unit, or protofilament. The protofilament is a double-strand of molecules having a twofold screw symmetry similar to the structure formed by the stacking of the crystallographic asymmetric unit along its *a*-axis.

A new fiber pattern was encountered during the course of recording the x-ray diffraction from pelleted deoxygenated sickle cell erythrocytes (Fig. 1). This pattern was recorded from a region adjacent to twinned triclinic HbS crystals and adjacent to the "classic" fiber (12). Of the hundreds of observed patterns, this was the first that differed significantly from the "classic" fiber pattern. Its layer line periodicity is 109 Å instead of 64 Å. From the differences in the diffraction patterns, it is obvious that the basic structural unit, the protofilament, of this newly observed fiber cannot be the same as the double-strand of the "classic" fiber. The packing of these protofilaments into a fiber also must differ. The unique molecular aggregation of HbS responsible for this pattern may exist in sickle cell erythrocytes, despite its low abundance, and the rare occurrence of its pattern.

Unlike the case of the "classic" fiber, where a crystalline structure served to identify the basic structural unit of the fiber (7, 8), no crystalline hemoglobin patterns comparable to patterns of the new fiber have been reported. In crystals of orthorhombic Hb Iwate (13) and deoxy-HbC (14), one of the cell dimensions is about the same as the fiber layer line periodicity of 109 Å. The *a*-axis dimension is 64 Å in these crystals, in the deoxy-HbS crystal, and in all unliganded human Hb crystals (15). In HbC, the substitution is glu-lys at the β6

Address correspondence to Beatrice Magdoff Fairchild.

0006-3495/92/06/1638/09 $2.00

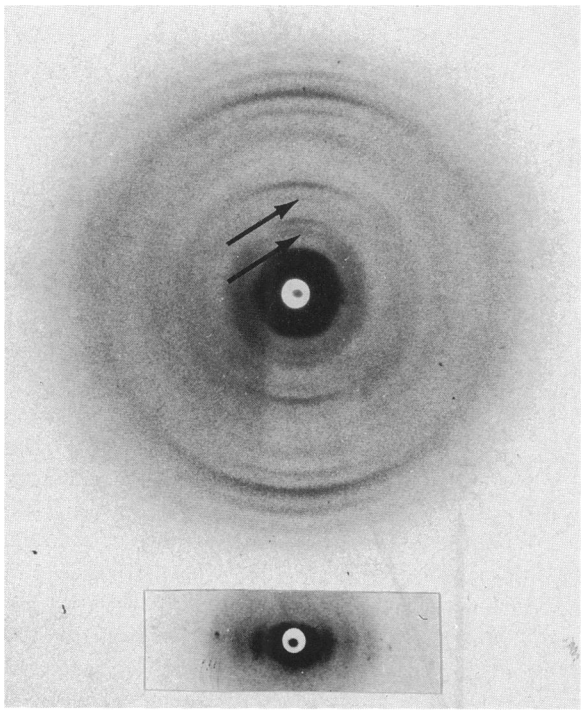

FIGURE 1 X-ray diffraction pattern of the new deoxy-HbS fiber with a layer line spacing of 109.41 Å. The arrows identify two diffraction maxima that may be attributed to the second and third layer lines of the "classic" fiber. The inset shows the equatorial reflections at (241, 121, 76, and 52 Å)$^{-1}$.

positions, compared with the substitution of glu-val at the same positions in HbS. Since there is no β6 substitution in Hb Iwate, only the deoxy-HbC crystal structure is of potential interest to these studies.

The two molecules of deoxy-HbC, related by the operation of a crystallographic twofold screw axis parallel to the 64 Å *a*-axis, stack along the axis to form a double-strand. In the deoxy-HbS monoclinic crystal, similar double-strands arise from the stacking of the two molecules in the asymmetric unit that are related by a noncrystallographic pseudo-screw axis. These double-strands are structurally the same as the "classic" fiber protofilaments. The intermolecular contacts that one of the substituted β6 residues, either val or lys, makes with its symmetry related neighboring molecule in the deoxy-HbS and deoxy-HbC crystals are similar. The other β6 of the Hb molecule does not participate in intermolecular contacts in either of these crystalline structures.

One important constraint for the new fiber computer model building is that one of the β6 residues participates in an intermolecular contact with a neighboring molecule resulting in a periodicity of 109 Å, and not 64 Å. The deoxy-HbC crystalline structure does not satisfy this constraint. In consequence, this crystal structure cannot serve as starting model despite the similarity in its *c*-dimension and the 109 Å layer line periodicity of the new fiber.

It should be possible to model a plausible fiber with the information available from the diffraction pattern and from considerations of structural stability based on energy calculations (16). Such an approach has proven successful in modeling oligomeric structures in which the individual components of the oligomeric complex were known from x-ray diffraction studies. For example, calculations of the association energy of Hb dimers into a tetramer in the liganded conformation yielded one structure that was in close agreement with the structure determined through x-ray diffraction studies. The unliganded structure determined by similar calculations, however, showed greater deviation from the known conformation. The complex of bovine trypsin and its inhibitor was calculated from energy considerations. After inclusion of appropriate constraints, one structure of the complex agreed closely with the structure found by x-ray diffraction studies.

Similar calculations, based on the layer line periodicity and the role played by the substituted residue, β6, in intermolecular contacts, should provide acceptable protofilament models for fiber model construction. The assembly of each energetically acceptable protofilament model into a fiber structure should satisfy the constraint that the transform of the fiber model would be comparable to the observed data with minimal differences. This constraint acts to further delimit the number of acceptable protofilament models that can be used in constructing fiber models. Similar calculations to find protofilaments, *ab initio,* of the "classic" fiber validate the approximations made in the search for new protofilaments and fiber models.

METHODS

Sample preparation and x-ray diffraction

Erythrocytes from sickle cell blood of a patient homozygous for SS in which the concentration of fetal hemoglobin was only 1–2% were ultracentrifuged to obtain a column of packed cells. Cells of medium to low density roughly taken from approximately the middle third of the column ensured the absence of reticulocytes and irreversibly sickled cells. Erythrocytes, at a hematocrit of ~30, rotating in a flask at ~1 cycle/s, were deoxygenated slowly with a flow of a humidified atmosphere of 95% N_2-5% CO_2 for ~16–18 h to insure more uniform fiber formation. The suspensions of deoxygenated erythrocytes were ultracentrifuged for 1 h at 250,000 *g*. Only the pelleted erythrocytes at the very bottom of the centrifuge tubes were packed anaerobically into thin walled capillaries by shear and sealed with hot wax for subsequent recording of x-ray diffraction patterns.

Nickel filtered Cu radiation from a microfocus generator, operated at 50 kV and 7 mA for 15 to 80 h, depending on the distance of

specimen to film, was used to obtain diffraction patterns. A defining pinhole of 100 μm served to collimate the x-ray beam.

Association energy calculations

Three approximations served to reduce the exceedingly lengthy energy calculations required to construct feasible protofilaments, and to construct a fiber of minimal association energies of packed protofilament. In the first approximation, a simplified protein model (17) is used in which each residue is replaced by a sphere whose center is on the line joining the α and β carbon atoms. With this strategy of substituting a single parameter for the atomic coordinates of each residue, the computing time is reduced by an order of magnitude. Energies of nonbonded van der Waals' interactions between residue pairs, and energies of residue-solvent interactions were determined for the simplified protein model from equations given by Levitt (17). The spherical radii of the twenty residues are taken from Wodak and Janin (18).

The hydrophobic contributions to the free energy of association are of prime importance for the stability of protein complexes, and depend on the reduction of the accessible surface area (ASA) in protein–protein or protein–ligand association. A linear correlation of 25 cal/mol/Å^2 exists between the hydrophobic free energy and the ASA (19, 20). In these calculations, an analytical approximation of the reduction of ASA that results from the contact between two residues is used (21, 22). Only residues on the protein surface were considered.

In order to effect manageable computations, electrostatic and hydrogen bonding energies that arise from protein–protein associations were omitted. It was assumed that in this approximation, the differences are small between electrostatic and hydrogen bonding energies of protein molecules in solution and in polymers. Interactions between proteins replace similar interactions between protein and solvent.

Coordinate system and model parameters

For protofilament model building, a coordinate system introduced by Levinthal et al. (23) was modified (Fig. 2) A local reference system, whose X-axis initially coincides with the molecular X-axis and the protofilament axis, is assigned to each of two molecules. The coordinate systems were parallel, and their respective origins were placed at the center of mass of each molecule. Molecule 1, the source molecule, was fixed at the origin of the reference system, $S-X_1,Y_1,Z_1$. The origin of the reference system of the target molecule, 2, $T-X_2,Y_2,Z_2$, was placed at (54.5,0,z) in the reference system of molecule 1. The value $x = 54.5$Å remained constant. The latitudes and longitudes of a surface residue in molecule 2 and of the line ST that connects the origins of the two local systems are (θ_2, ϕ_2) and (θ_0, ϕ_0), respectively.

Molecule 2 was rotated about X_2 to through an angle $\Delta\phi = (\phi_0 - \phi_2)$ followed by a second rotation about Y_2 of $\Delta\theta = (\theta_0 - \theta_2)$, so that a surface residue of molecule 2 whose latitude and longitude are (θ_2, ϕ_2) would coincide with the line ST after these rotations. The final orientation of molecule 2 was then completed by a spin about the line ST through an angle of χ. The orientation of molecule 1 was obtained from that of molecule 2 for each orientation by the operation of twofold screw symmetry where the twofold axis is parallel to the fiber axis at $Y = 0$, $Z = z/2$ with respect to the reference system $S-X_1$, Y_1, Z_1. Because of the screw symmetry of the two molecules, the number of parameters that define the relative orientations and positions of the two HbS molecules are reduced from six to four; the independent variable parameters are z, θ_2, ϕ_2 and χ.

The parameter z was varied from 14 to 28 Å in steps of 2 Å, θ_2, from 0° to 180° in steps of 5°, ϕ_2, from 0 to 360° in steps of 10°, and χ from 0° to 360° in increments of 5°. In a finer search, the translational and angular steps were reduced to 0.5 Å and 1°. The simplified protein model of HbS was constructed from the atomic coordinates of the refined deoxy-HbS crystal structure at 2.8 Å resolutions (11) deposited in the Protein Data Bank (24). Only residues on the surface of the molecule were used whose distances from the molecular center of mass are greater than 20 Å and whose ASA values are nonzero.

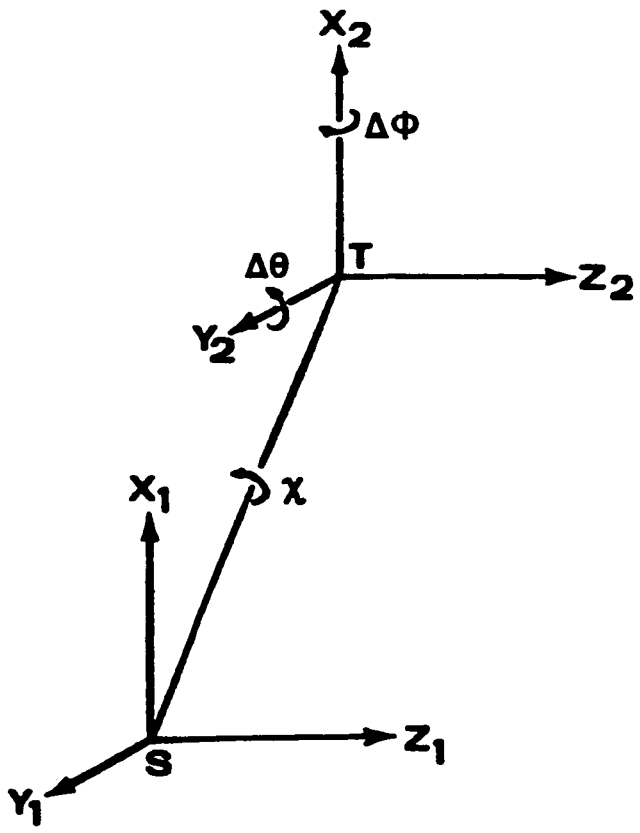

FIGURE 2 The local reference systems assigned to the source molecule, $S\text{-}X_1,Y_1,Z_1$, and to the target molecule, $T-X_2,Y_2,Z_2$. The origin of the first system was placed at the center of mass of the source molecule and its X-axis was taken parallel to the fiber axis. The origin of the second system, whose axes parallel those of the source system, coincides with the center of mass of the target molecule. It was positioned initially at (54.5, 0, z) in the first system. The latitude and longitude of a surface residue of the target molecule and the line ST joining the origins of the two systems are (θ_2, ϕ_2) and (θ_0, ϕ_0), respectively. The target molecule was rotated by $\Delta\phi = \phi_0 - \phi_2$ about X_2 followed by a rotation of $\Delta\theta = \theta_0 - \theta_2$ about Y_2, and then by a spin rotation around the line ST through an angle χ. The orientation of the source molecule was obtained by the operation of twofold screw symmetry on the target molecule after each set of rotations. A protofilament model was thus characterized by four parameters, z, θ_2, ϕ_2 and χ.

Calculation of Fourier transforms

Transforms of fiber models were calculated for comparisons with the observed data. Crystalline rather than Fourier-Bessel transforms were used. The advantage gained by this procedure is that changes in

translational parameters can be accomplished through the multiplication of a previously calculated transform by a phase factor, i.e., an exponential, $\exp(-2\pi iH \cdot \Delta r)$, where H is equal to (hkl) and Δr is the change in positional parameter. This technique was used previously to explore transforms of the "classic" fiber models (25, 26). The unit cell was taken with $a = 109$ Å along the fiber axis, and with $b = 400$ Å and $c = 400$ Å for the cross-sectional dimensions. The latter values are sufficiently large to ensure that the transform is sampled at small enough intervals. The disorientation of the fiber was taken into account by smearing the transforms of the near-meridional reflections by a Gaussian of 5° half width.

The observed intensity I_0 was obtained from a scan of the diffraction film (Fig. 1) along the meridian after correcting for polarization and Lorentz factors (27). The summation of contributions of the squared structure factors extending to a value of <0.02 Å^{-1} along the layer line served as the calculated intensity at the meridian.

The R-factor was computed by $R = \Sigma |I_0 - kI_c| / \Sigma I_0$, where symbols I_0 and I_c denote the observed and calculated intensities at reciprocal distances measured from the meridian, equivalent to the points at which the film was digitized, and where k is the scale factor. In computing I_c, the atomic scattering factors were corrected for the aqueous solvent contribution (28).

CONSTRUCTION OF PROTOFILAMENTS

Constraints on protofilament models

(*a*) The stacking of the HbS molecules related by a twofold screw axis with a translational component of 54.5 Å describes a protofilament that accounts for the observed periodicity of 109 Å, determined from measurements of seven medium to strong meridional or near-meridional reflections of the fiber pattern (Fig. 1, Table 1). At least two molecules are needed to satisfy the requirement of the layer line periodicity because the maximum dimension of the Hb molecule is 64 Å.

The twofold screw symmetry becomes a necessary constraint for the construction of protofilaments. Release of this constraint entails the expansion of protofilament computer model building from a four-dimensional to a six-dimensional search in space, requiring very lengthy computations. An increased number of energetically favorable protofilament models would result. This would lead to a greater number of searches for acceptable fiber models. In turn, these models would require additional constraints that cannot be imposed because of the limited data.

(*b*) At least one of the two substituted β6 residues in HbS should participate in intermolecular contacts in the protofilament. This restraint supports the assumption that protofilament and fiber formation occur as a result of the presence of the substituted hydrophobic residue.

(*c*) The association energy of molecules into a protofilament should be a minimum with a value equal to or lower than −24 kcal/mol. This value is comparable to the molecular association energy of the asymmetric unit of the monoclinic crystal structure, which serves as a protofilament model for the "classic" fiber.

Protofilament models

A search for a protofilament that satisfies the above constraints has yielded 12 models (Table 2) out of the 746,496 investigated. Latitudes and longitudes of the surface residues of molecule 2 in contact with the β6 residue of the β_2 chain in molecule 1 are shown in Fig. 3 for each of the 12 protofilament models, and are numbered to correspond to those in Table 2. All 12 protofilament models of the new HbS fiber consist of zigzag mono-strands similar to protofilament PF-1 (Fig. 4 *a*). These protofilaments differ markedly from the double-strand of the "classic" fiber (Fig. 4 *b*).

Searches for protofilament structures of the "classic" fiber through association energy calculations

The justification for the use of a simplified protein model in exploring new protofilament models through energy calculations was sought by comparison to results

TABLE 1 Layer line spacings of the new HbS fiber diffraction pattern

Spacing (Å)	Layer Line*	Periodicity‡ (Å)
27.51	4	110.04
18.19	6	109.14
12.25	9	110.25
10.84	10	108.40
10.00	11	110.00
9.08	12	108.96
8.39	13	109.07

*Layer lines 5, 7, and 8 are absent or diffuse. ‡Periodicity is 109.4 ± 0.7 Å.

TABLE 2 Parameters and energy of protofilament models

No.	z (Å)	ϕ_2^0	θ_2^0	χ^0	E kcal/mol
PF-1	20.0	191	22	91	−24.5
PF-2	20.0	184	58	128	−24.4
PF-3	13.0	140	67	160	−28.3
PF-4	14.25	127	62	204.5	−31.1
PF-5	15.5	91	64	229	−24.3
PF-6	17.25	61	57	209	−31.3
PF-7	16.5	54	65.5	247.5	−27.2
PF-8	16.0	62	47	290	−24.6
PF-9	13.5	71	50	308	−25.7
PF-10	15.5	89	24	305	−26.6
PF-11	22.0	27	18	298	−26.5
PF-12	27.0	274	32	155	−25.7

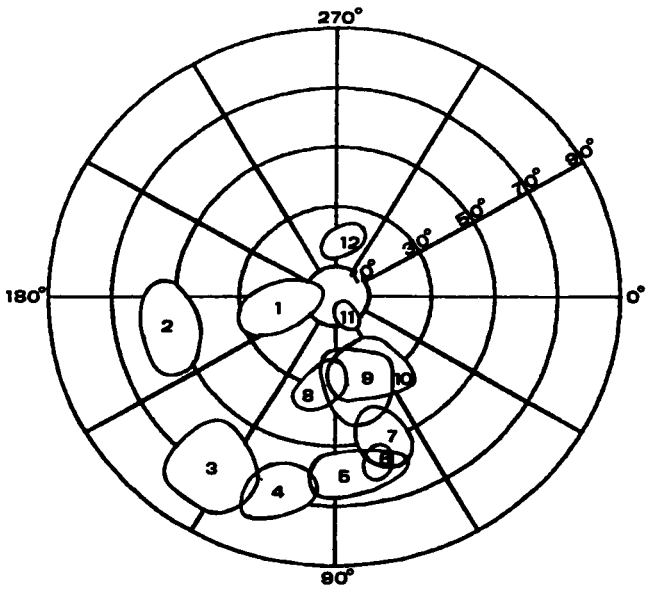

FIGURE 3 A polar plot of contact regions on the surface of the target molecule for the 12 protofilament models in Table 2. The numbered regions correspond to the model numbers in Table 2. In 11 of the 12 protofilament models, surface residues of α chain in the target molecule are in contact with β6 of the β_2 chain of the source molecule; in protofilament model PF-12, the β chain of target molecule interacts with β6 of the source molecule.

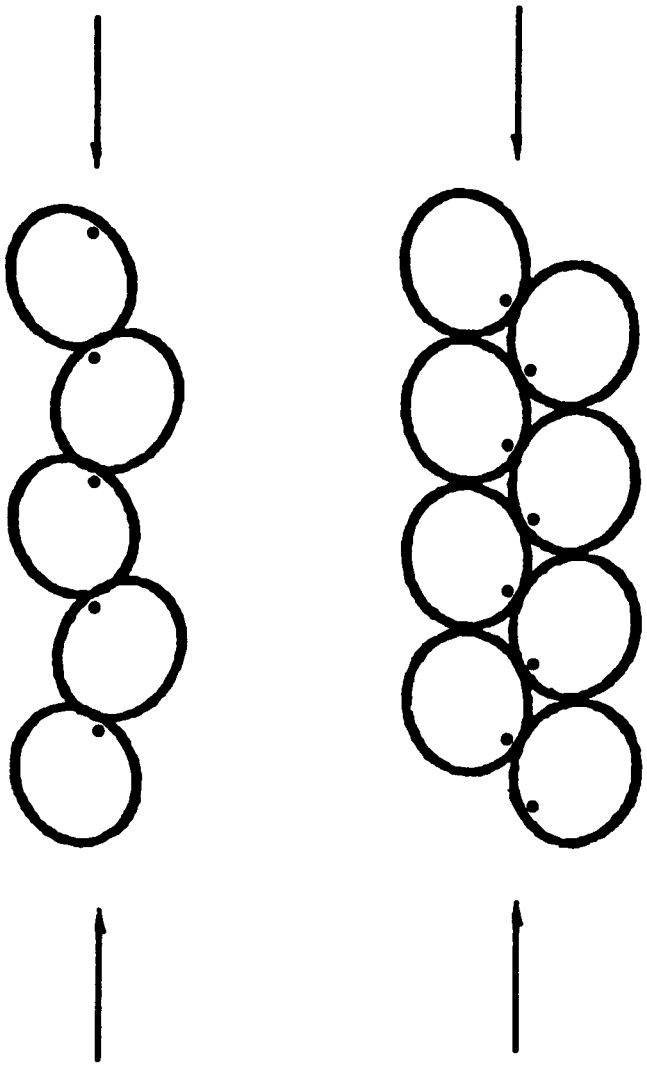

FIGURE 4 (*a*) (*left*) The zigzag mono-strand protofilament model of the new HbS fiber contrasted with (*b*) (*right*) the double-strand protofilament of the "classic" fiber. The β6 contacts are marked by a dot. Note that there are both lateral and axial contacts between molecules in the protofilament of the "classic" fiber and there are only axial contacts in any of the protofilament models of the new fiber.

of systematic searches for protofilament structures of the "classic" fiber. For these calculations, spheres replaced the surface residues (16, 17) of the two molecules in the crystalline asymmetric unit. Their centers of mass were positioned as reported for the crystalline unit cell (9). The two molecules of the asymmetric unit were related by an exact twofold screw symmetry along the direction of the crystalline *a*-axis as contrasted with the near-screw symmetry that occurs in the crystal.

The three orientational parameters of the two molecules were changed over their entire range in small increments. Out of 11,664 models investigated, three showed a minimum energy lower than −24 kcal/mol and included a β6 valine contact between the molecules. One of the models is similar to the asymmetric unit of the crystalline deoxy-HbS; the orientational parameters differ by 6° in θ_2, 1° in ϕ_2, and 4° in χ.

The close similarity of the protofilament structure of the "classic" fiber, based on the asymmetric unit of the crystal structure, and one of the three protofilament models derived *ab initio* from energy calculations made with the use of the above approximations, support these procedures as a means for establishing stable protofilament models. Furthermore, a value of −24 kcal/mol, initially chosen as the maximum permissible association energy of two neighboring molecules into a protofilament of the new fiber, is reasonable. This value of −24 kcal/mol is the same for the intermolecular lateral association energy needed to form the protofilament of the "classic" fiber.

FIBER MODELS

The equatorial reflections (Fig. 1, *inset*) show that the protofilaments pack pseudohexagonally. The $(241\ \text{Å})^{-1}$ reflection accounts for the interfiber distance, and places a limit on the maximum dimensions of the fiber cross-

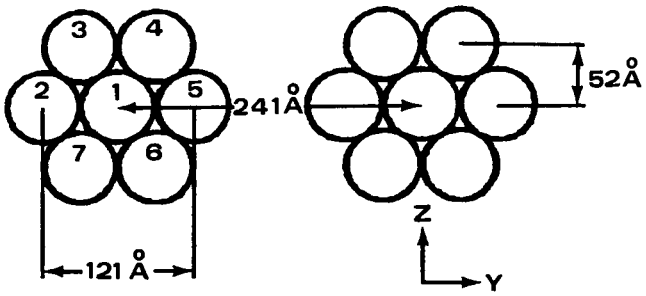

FIGURE 5 The view down the **X**-axis (fiber axis) of a plausible hexagonal packing of protofilaments of the new HbS fiber. Three of the four equatorial reflections (*inset*, Fig. 1) were consonant with the distances shown in this figure. The fourth reflection may be associated with an interprotofilament distance. The reflection at $(241\ Å)^{-1}$ places a limit on the maximum fiber diameter. The protofilaments in the fiber models are numbered as shown here.

section. Reflections at $(52\ Å)^{-1}$ and $(121\ Å)^{-1}$ define interprotofilament distances (Fig. 5). The $(76\ Å)^{-1}$ reflection also may be associated with an interprotofilament distance. A seven protofilament assembly (Fig. 5) could serve as a fiber model.

Because of the limited data, approximations are necessary in order to calculate an acceptable fiber model. The basic unit of the fiber is taken to comprise four protofilaments, 1–4 in Fig. 5 *a*. A hexagonally packed fiber model consisting of seven protofilaments, derived from the basic unit by appropriate protofilament translations of 121 Å along the **Y**-axis or 102 Å along the **Z**-axis, may be constructed with seven variable parameters; three establish the relative heights of the four protofilaments, and four establish the rotation angle about each protofilament axis. The 10 meridional, or near-meridional, intensities of layer lines 4 through 13 depend mainly on the relative heights, while the total energy of protofilament packing into a fiber depends on both the heights and the angular parameters.

Systematic searches were undertaken to find fiber models whose *R*-factors and packing energies are minimal. Each of the 12 protofilament models (Table 2) was used in a search for an acceptable fiber model. The range of relative heights was varied between −30 and +30 Å, and the angular parameters between 0° and 360°. Only protofilaments PF-1 and PF-8 yielded satisfactory models (Table 3). The molecular packing in fiber models FM-1 and FM-3 are shown in Fig. 6.

Table 4 lists the interprotofilament contacts for model FM-3; those for FM-1, and FM-2, and FM-4 are not included but are available upon request. For simplicity and clarity, the standard notation for the structural regions of the hemoglobin molecule (29) is used in the location of residues. A molecule in a fiber packing model is denoted by three digits; the first of which assigns the protofilament (Fig. 5); the second, molecule 1 or 2 in the repeat unit along fiber axis; and the third, the translational mate along the **X**-axis. For example, molecule 121 denotes a target molecule, 2, in protofilament 1 translated by 109 Å along the positive direction of the **X**-axis, and molecule $71\bar{1}$ specifies a source molecule, 1, in protofilament 7 translated by 109 Å along the negative **X**-axis direction. Note that residues from the heme pocket (helical regions **E, F, F** and the nonhelical region **EF**) participate in all interprotofilament contacts.

DISCUSSION

The fiber pattern shown in Fig. 1 may be compared to the pattern of the "classic" fiber (7). In both patterns, significant diffraction maxima are present mainly on or near the meridian. The intensity of the 14th layer line near-meridional reflection of 109 Å periodicity, at 8 Å resolution, on the new fiber pattern is medium to strong; and similarly, on the "classic" fiber pattern, a medium to strong maximum appears on the 13th layer line of the 64 Å periodicity, at 5 Å resolution. The high resolution along the fiber axis, in both patterns, is associated with a highly ordered stacking of the HbS molecules. The equatorial reflections indicate that the interfiber distances are ~240 Å, somewhat larger than the value of 220 Å found for the "classic" fiber. These prominent features of the pattern suggest that the helical repeat is

TABLE 3 **Positional* and rotational parameters of acceptable fiber models; their minima *R*-factors and energies**

Model	Positional parameters (Å)					Rotational parameters (°)				*R*-Factors	Energy	Protofilament
No.	*x*(2)	*x*(3)	*x*(4)	−*y*	*z*	*ra*(1)	*ra*(2)	*ra*(3)	*ra*(4)		kcal	No.
FM-1	−1	−5	−5	59	50	−7	5	−6	−6	0.218	−133	PF-1
FM-2	0	4	−4	60	50	35	35	45	46	0.216	−93	PF-1
FM-3	4	−20	−16	58	50	115	111	91	95	0.207	−130	PF-1
FM-4	14	20	−6	61	52	180	147	140	175	0.235	−64	PF-8

*The *x* parameters correspond to the heights of protofilament 2, 3, and 4 as shown in Fig. 5. The height of protofilament 1 was arbitrarily taken at zero.

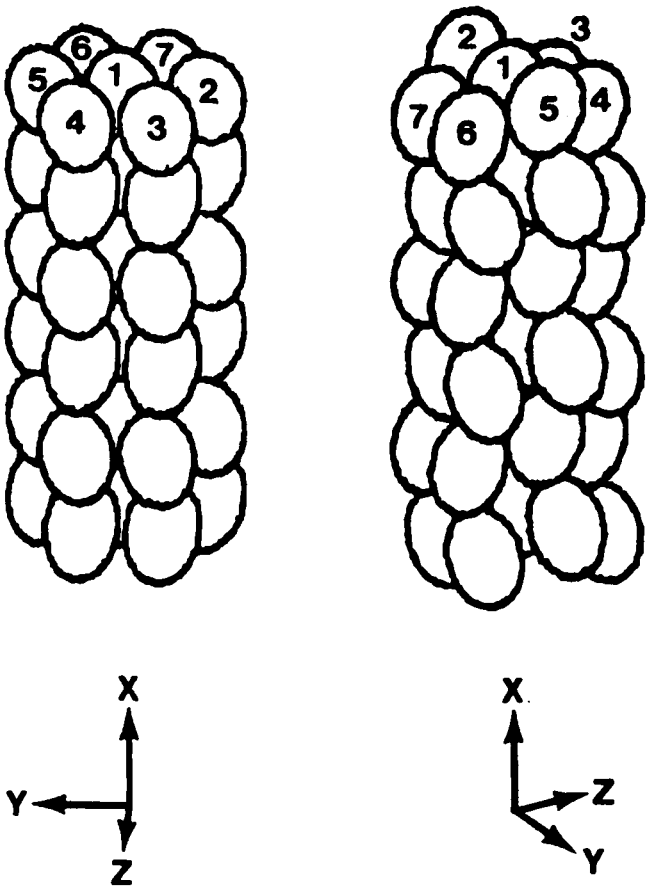

FIGURE 6 The packing of HbS molecules in FM-1 (*a*) (*left*) and in FM-3 (*b*) (*right*). The HbS molecule is represented by an ellipse. Both models are near-layered structures in which the molecules are pseudo-hexagonally packed. In *a*, model FM-1, the molecular layer is perpendicular to the fiber axis, **X**. In *b*, by contrast, the molecular layers in FM-3 are perpendicular to the **Z** direction and parallel to the fiber axis. The molecular packing in FM-3 is more dense than in FM-1.

very large, and may be similar to the ~50 molecule helical repeat of the "classic" fiber (4).

Additional comparisons of the patterns indicate the presence of low concentrations of the "classic" fiber that may be associated with the new fiber. Near-meridional reflections at (32 and 21 Å)$^{-1}$ on the new fiber pattern (*arrows*, Fig. 1) could not be indexed on the basis of 109Å periodicity, but might be the second and third layer line reflections of the "classic" fiber. This is not surprising because the new fiber was found in the same capillary adjacent to an unusual triclinic crystal of deoxy-HbS (12) comprising double-strands comparable to the asymmetric unit of the monoclinic crystal, and whose diffraction pattern along the a^*-axis is similar to the pattern of the monoclinic crystal and the "classic" fiber.

Traces of what might be new fiber diffraction was detected in the "classic" fiber pattern. The strong diffuse scattering that is always observed in the 10 Å region of the "classic" fiber has no counterpart in the deoxy-HbS crystalline structure that consists of double-strands equivalent to the "classic" fiber protofilament. Even on a smeared rotation diagram of the crystal, no diffraction maxima appear at ~10 Å (Fig. 2, reference 7). The diffuse scattering in patterns of the "classic" fiber may be due to the 11th order near-meridional reflection at 10 Å of the new fiber, which is the second most intense maximum on the pattern. The new fiber, poorly or even randomly oriented, may be present in low concentrations.

The methods of energy calculations and the approximations introduced by the use of a simplified protein model, an analytical expression of the accessible surface area, and the omission of electrostatic and hydrogen bonding energies are acceptable in searches for new protofilament and fiber models.

The same approximations served in the calculations for finding the orientation and juxtaposition of two HbS molecules related by twofold screw symmetry with a translational repeat of 32 Å. The results were compared to the deoxy-HbS crystalline asymmetric unit determined by *x*-ray diffraction studies (9–11). One out of the three acceptable models corresponds to the correct structure of the asymmetric crystalline unit, and in turn to the protofilament structure of the "classic" fiber. The selection of a unique model, which is of general interest but of no special concern to this work, may become possible with the use of additional conditions and constraints. These calculations, however, confirm that the constraints, choice of association energy maximum, and the simplifying assumptions are adequate to lead to a correct model.

The diffraction pattern of the new fiber in conjunction with energy calculations of molecular assembly were used as determining factors in protofilament and fiber construction. The periodicity of 109 Å (Table 1) and a molecular association energy of < -24 kcal/mol serves to establish 12 possible mono-strand protofilament structures (Table 2 and Fig. 3). The equatorial reflections, besides establishing the cylindrically averaged cross-sectional dimension of the fiber, show the near-hexagonal packing of protofilaments into a fiber. Finally, the intensities of the 10 meridional reflections and the packing energy calculations provide a means of determining the relative heights and the rotational disposition of the protofilaments when assembled into a fiber.

TABLE 4 **Interprotofilament contacts of fiber model FM-3**

Interacting molecules*		Chain No.	Contact regions on molecule I‡	Chain No.	Contact regions on molecule II‡
I	II				
110	521	α_1:	A(6), E(1)	α_2:	A(1), B(3), D(2), E(2)
110	210	β_2:	EF(1), F′(1)	α_2:	E(3)
110	410	α_1:	F′(1), F(1)	β_1:	E(1), F′(1)
110	610	β_1:	CD(3), D(2), E(3)	β_2:	E(4), F(2)
110	710	β_1:	A(8), B(2), E(6), EF(1)	β_2:	CD(4), D(4), E(3)
110	420	α_2:	G(3)	α_1:	CD(1), D(1), E(1), F(1)
		β_2:	B(1), D(2)		
120	210	α_1:	A(6), E(1)	α_2:	A(1), B(3), D(2), E(2)
120	320	β_1:	CD(2)	β_2:	E(2)
120	420	β_1:	A(6), B(1), E(10), EF(1)	β_2:	CD(4), D(5), E(3)
120	520	β_2:	EF(1), F′(1)	α_2:	E(3)
120	720	α_1:	F′(1)	β_1:	E(1)
120	711	α_2:	G(3), GH(2)	α_1:	CD(3), D(1), E(2), F(3)
		β_2:	A(1), B(4), D(3), E(2), G(1)	α_2:	C(1), FG(1)
210	710	β_1:	CD(1)	β_2:	E(2)
210	320	α_2:	G(3), GH(2)	α_1:	C(1), CD(3), D(2), F(3)
		β_2:	A(1), B(1), D(1), E(1)	β_2:	C(1), CD(1)
210	720	α_2:	CD(1)	β_1:	CD(1), D(4)
410	521	β_1:	D(2)	α_2:	CD(1)
410	310	β_1:	E(2), EF(2)	α_2:	E(3), EF(1)
610	521	α_1:	CD(2), D(1), E(2), F(3)	α_2:	G(3), GH(2)
		β_2:	C(1)	β_2:	A(1), B(2), CD(2), E(1)
610	510	β_2:	CD(4), D(5), E(3)	β_1:	A(8), B(2), E(7), EF(1)
610	710	β_1:	E(2), EF(2)	α_2:	E(3), EF(1)
220	320	β_1:	A(8), B(2), E(2)	β_2:	CD(4), D(4), E(2)
420	320	α_2:	E(1), EF(1)	β_1:	E(1), EF(1), F′(1)
420	520	β_2:	E(3), F(1)	β_1:	CD(2), D(2)
420	311	α_2:	A(6), B(2), G(1)	α_1:	A(2), E(9), EF(2)
620	720	α_2:	E(1), EF(1)	β_1:	E(1), EF(1), F′(1)
620	711	α_2:	A(6), B(2), G(1)	α_1:	A(2), E(9), EF(2)

*First digit in columns 1 and 2 refers to protofilament number (Figs. 5 and 6), second digit to source (1) or target (2) molecule, and third to their respective molecular translation along the fiber axis in units of 109 Å. ‡Numbers in parenthesis indicate the number of contact residues.

Of the 12 protofilament models that satisfy the constraints, only two, PF-1 and PF-8, form acceptable fiber models (Table 3). Their *R*-factors are almost the same and, as a result, one fiber model cannot be selected as significantly better than any of the other models. Some preference may be given to the choice of a fiber model formed by protofilament PF-1. The packing densities of the protofilaments in the fiber models with protofilament PF-1 are between 1 to 5% lower than the packing density of the deoxy-HbS crystalline structure. By contrast, model FM-4 has a packing density that is ~10% lower. Moreover, the energy of protofilament association is higher for model FM-4.

The hydrophobic heme pocket **F-EF-F′-F** constitutes a region of interprotofilament interactions in fiber model FM-3 (Table 4), and in the other three models as well (not listed). Thus, the interstrand interactions in the new fiber are similar to the lateral intermolecular interactions of the double-strand in the "classic" fiber. The heme pocket plays an important role in the assembly of the strands of the new HbS fiber, and in the assembly of the "classic" fiber protofilaments and in crystalline deoxy-HbS.

The available information is insufficient to assess the role that this new fiber may play in the sickling of erythrocytes. Further work is needed.

We thank Drs. Philip E. Bourne of the Howard Hughes Medical Institute, Columbia University, College of Physicians and Surgeons, for valuable discussions and access to the Convex computer, L. S. Rosen for some of the preliminary programs used in the construction of protofilament models, and John F. Bertles for continuing support and encouragement.

This work was supported by the National Institutes of Health grant HL-23984.

Received for publication 27 August 1991 and in final form 16 December 1991.

REFERENCES

1. Perutz, M. F., and J. M. Mitchison. 1950. State of haemoglobin in sickle-cell anemia. *Nature (Lond.).* 166:677–679.
2. Magdoff-Fairchild, B., W. N. Poillon, T. L. Li, and J. F. Bertles. 1976. Thermodynamic studies of polymerization of deoxygenated sickle cell hemoglobin. *Proc. Nat. Acad. Sci. USA.* 73:990–994.
3. Hofrichter, J., P. D. Ross, and W. A. Eaton. 1976. Supersaturation in sickle cell hemoglobin solutions. *Proc. Nat. Acad. Sci. USA.* 73:3035–3039.
4. Dykes, G. W., R. H. Crepeau, and S. J. Edelstein. 1979. Three-dimensional reconstruction of the 14-filament fibers of hemoglobin S. *J. Mol. Biol.* 130:451–472.
5. Rodgers, D. W., R. H. Crepeau, and S. J. Edelstein. 1987. Pairing and polarities of the 14 strands in sickle cell hemoglobin fibers. *Proc. Nat. Acad. Sci. USA.* 84:6157–6161.
6. Carragher, B., D. A. Bluemke, B. Gabriel, M. J. Potel, and R. Josephs. 1988. Structural analysis of polymers of sickle cell hemoglobin. I. Sickle hemoglobin fibers. *J. Mol. Biol.* 199:315–331.
7. Magdoff-Fairchild, B., and C. C. Chiu. 1979. X-ray diffraction studies of fibers and crystals of deoxygenated sickle cell hemoglobin. *Proc. Nat. Acad. Sci. USA.* 76:223–226.
8. Magdoff-Fairchild, B., C. C. Chiu, and J. F. Bertles. 1981. The structure of fibers in sickled erythrocytes. *In* The Molecular Basis of Mutant Hemoglobin Dysfunction. P. B. Sigler, editor. Elsevier/North Holland Biomedical Press, Amsterdam. 125–136.
9. Wishner, B. C., K. B. Ward, E. E. Lattman, and W. E. Love. 1975. Crystal structure of sickle-cell deoxyhemoglobin at 5 Å resolution. *J. Mol. Biol.* 98:179–194.
10. Wishner, B. C., J. C. Hanson, W. M. Ringle, and W. E. Love. 1975. Crystal structure of sickle-cell deoxyhemoglobin. *In* Proceedings of the Symposium on Molecular and Cellular Aspects of Sickle Cell Disease. J. I. Hercules, G. L. Cottam, M. R. Waterman, and A. N. Schechter, editors. DHEW Publication No. (NIH) 76-1007. 1–29.
11. Padlan, E. A., and W. E. Love. 1985. Refined crystal structure of deoxyhemoglobin S. 1. Restrained least-squares refinement at 3-Å resolution. *J. Biol. Chem.* 260:8272–8279.
12. Magdoff-Fairchild, B., L. S. Rosen, and C. C. Chiu. 1982. Triclinic crystals associated with fibers of deoxygenated sickle hemoglobin. *EMBO. J.* 1:121–126.
13. Greer, J. 1971. Three dimensional structure of abnormal human hemoglobins M Hyde Park and M Iwate. *J. Mol. Biol.* 59:107–126.
14. Fitzgerald, P. M. D., and W. E. Love. 1979. Structure of deoxy hemoglobin C (beta six Glu→Lys) in two crystal forms. *J. Mol. Biol.* 132:603–619.
15. Frier, J. A., and Perutz, M. F. 1977. Structure of human foetal deoxyhaemoglobin. *J. Mol. Biol.* 112:97–112.
16. Wodak, S. J., M. deCrombrugghe, and J. Janin. 1987. Computer studies of interactions between macromolecules. *Prog. Biophys. Mol. Biol.* 49:29–63.
17. Levitt, M. 1976. A simplified representation of protein conformations for rapid simulation of protein folding. *J. Mol. Biol.* 104:59–107.
18. Wodak, S. J., and J. Janin. 1978. Computer analysis of protein-protein interactions. *J. Mol. Biol.* 124:323–342.
19. Chothia, C. 1974. Hydrophobic bonding and accessible surface area in proteins. *Nature (Lond.).* 248:338–339.
20. Chothia, C. 1975. Structural invariants in protein folding. *Nature (Lond.).* 254:304–308.
21. Wodak, S. J., and J. Janin. 1980. Analytical approximation to the accessible surface area of proteins. *Proc. Nat. Acad. Sci. USA.* 77:1736–1740.
22. Wodak, S. J., and J. Janin. 1981. Location of structural domains in proteins. *Biochemistry.* 20:6544–6552.
23. Levinthal, C., S. J. Wodak, P. Kahn, and A. K. Davidanian. 1975. Hemoglobin interaction in sickle cell fibers. I. Theoretical approaches to the molecular contacts. *Proc. Nat. Acad. Sci. USA.* 72:1330–1334.
24. Bernstein, F. C., T. F. Koetzle, G. F. H. Williams, E. F. Meyer, Jr., M. D. Bride, J. P. Rogers, O. Kennard, T. Shimanouche, and M. Tasumi. 1977. The protein data bank: a computer based archival file for macromolecular structures. *J. Mol. Biol.* 112:535–542.
25. Rosen, L. S., and B. Magdoff-Fairchild. 1985. X-ray diffraction studies of 14-filament models of deoxygenated sickle cell hemoglobin fibers. Models based on electron micrograph reconstructions. *J. Mol. Biol.* 183:565–574.
26. Rosen, L. S., and B. Magdoff-Fairchild. B. 1988. X-ray diffraction studies of 14-filament models of deoxygenated sickle cell hemoglobin fibers. II. Models based on the deoxygenated sickle hemoglobin crystal structure. *J. Mol. Biol.* 200:141–150.
27. Fraser, R. D. B., and T. P. McRae. 1973. Conformation in Fibrous Proteins. Academic Press, New York. 628 pp.
28. Fraser, R. D. B., T. P. McRae, and E. Suzuki. 1978. An improved method for calculating the contribution of solvent to the X-ray diffraction pattern of biological molecules. *J. Appl. Cryst.* 11:693–694.
29. Perutz, M. F., M. G. Rossman, A. F. Cullis, H. Muirhead, G. Will, and A. C. T. North. 1960. Structure of haemoglobin. A three-dimensional Fourier synthesis at 5.5 Å resolution obtained by X-ray analysis. *Nature (Lond.).* 185:416–422.